The Effect of Soil Thermal Conductivity Parameterization on Surface Energy Fluxes and Temperatures

C. D. Peters-Lidard

Civil and Environmental Engineering, Georgia Institute of Technology, Atlanta, Georgia

E. Blackburn, X. Liang, and E. F. Wood

Water Resources Program, Princeton University, Princeton, New Jersey

(Manuscript received 8 July 1996, in final form 3 April 1997)

ABSTRACT

The sensitivity of sensible and latent heat fluxes and surface temperatures to the parameterization of the soil thermal conductivity is demonstrated using a soil vegetation atmosphere transfer scheme (SVATS) applied to intensive field campaigns (IFCs) 3 and 4 of the First ISLSCP (International Satellite Land Surface Climatology Project) Field Experiment (FIFE). In particular, the commonly used function for soil thermal conductivity presented by M. C. McCumber and R. A. Pielke results in overestimation during wet periods and underestimation during dry periods, as confirmed with thermal conductivity data collected at the FIFE site. The ground heat flux errors affect all components of the energy balance, but are partitioned primarily into the sensible heat flux and surface temperatures in the daytime. At nighttime, errors in the net radiation also become significant in relative terms, although all fluxes are small. In addition, this method erroneously enhances the spatial variability of fluxes associated with soil moisture variability. The authors propose the incorporation of an improved method for predicting thermal conductivity in both frozen and unfrozen soils. This method requires the specification of two additional parameters, and sensitivity studies and tables of recommended parameter values to facilitate the incorporation of this method into SVATS are presented.

1. Introduction

The partitioning of water and energy fluxes at the land surface has received much attention in both the numerical weather prediction (NWP) and global climate modeling communities and is the subject of a major international effort known as PILPS (The Project for Intercomparison of Land Surface Parameterization Schemes) (Henderson-Sellers et al. 1995). Studies motivating this project have shown that prediction of accurate sensible and latent heat fluxes as well as surface temperature and moisture are critical for predicting convection, clouds, and air temperature and moisture at a variety of temporal and spatial scales (e.g. Walker and Rowntree 1977; Shukla and Mintz 1982; Avissar and Pielke 1989; see also the reviews of Avissar and Verstraete 1990 and Garratt 1993).

The datasets of the FIFE experiment (Sellers et al. 1992; Strebel et al. 1994) have provided valuable validation criteria for the newest generation of land surface energy and water balance models or soil vegetation atmosphere transfer schemes (SVATS). Two recent works that make use of the FIFE data relate to efforts at the European Centre for Medium-Range Weather Forecasts (ECMWF) (Viterbo and Beljaars 1995) and the National Centers for Environmental Prediction (NCEP, formerly the National Meteorological Center) (Chen et al. 1996).

These efforts are illustrative of the recent trend toward improving soil hydraulics in SVATS (see also Cuenca et al. 1996) while retaining simpler, historically favored formulations of soil thermodynamics.

We present a review of the representation of soil thermal conductivity in SVATS, with the goals of 1) illustrating the sensitivity of surface fluxes and temperatures to this representation, and 2) proposing a new method for predicting thermal conductivity in SVATS. Application of our proposed method for predicting thermal conductivity to FIFE intensive field campaigns (IFCs) 3 and 4 and comparisons to the McCumber and Pielke (1981) method illustrate the significant effects of this parameterization on the surface energy balance.

2. Representation of soil thermal conductivity

In this section we present a brief description of soil thermodynamics in SVATS and methods for representing soil thermal conductivity. For a comprehensive re-

Corresponding author address: Christa Peters-Lidard, School of Civil and Environmental Engineering, Georgia Institute of Technology, Atlanta, GA 30332-0355.
E-mail: cpeters@ce.gatech.edu

TABLE 1. Thermal properties of soil constituents (after Farouki 1986).

Material	Density $\begin{pmatrix} \times10^3 \\ \text{kg m}^{-3} \end{pmatrix}$	Specific heat (J kg^{-1} K^{-1})	Heat capacity $\begin{pmatrix} \times10^3 \\ \text{J K}^{-1}\text{ m}^{-3} \end{pmatrix}$	Thermal conductivity (W m^{-1} K^{-1})
Quartz	2.65	733	1942	8.4
Soil minerals	2.65	733	1942	2.9
Soil organics	1.30	1926	2503	0.25
Water	1.00	4186	4186	0.6
Ice	0.90	2093	1883	2.5
Air	0.0012	1005	1.20	0.026

view of soil thermodynamics, the reader is referred to

pared only three soil types—clay, silt loam, and fine sand. In addition, there is no information in AK65 regarding experimental standard deviations or the applicability to frozen soils. Because this relationship is dependent on the soil water potential, it implicitly depends on the choice of the soil water retention function, and any uncertainty in its associated parameters as Cuenca et al. (1996) discuss.

The MP81 method is used by numerous SVATS including Noilhan and Planton (1989), Ek and Mahrt (1991), Famiglietti and Wood (1994a), Xinmei and Lyons (1995), Viterbo and Beljaars (1995), and Chen et al. (1996).

b. Johansen (1975)

As previously discussed, Farouki (1986) concluded that for fine unfrozen soils, or for fine or coarse frozen soils, the Johansen (1975) method was the most accurate over the full range of saturation, with deviations within the 35% range for saturation over 0.2. For saturations under 0.2, Farouki indicates that Johansen's original method underestimates thermal conductivity by about 5%–15%, and therefore he recommends a slightly modified method in these situations. This modified method is presented below.

J75 calculates the thermal conductivity of a soil as a function of its saturation, porosity, quartz content, and dry density and phase of water (frozen or unfrozen). The method thus requires more parameters than the MP81 approach. Johansen calculates thermal conductivity κ as a combination of the dry κ_{dry} and saturated κ_{sat} thermal conductivities, weighted by a normalized thermal conductivity (K_e, known as the Kersten number):

$$\kappa = K_e(\kappa_{sat} - \kappa_{dry}) + \kappa_{dry}. \tag{5}$$

The method consists of four steps: 1) determine the dry thermal conductivity, 2) determine the saturated thermal conductivity, 3) determine the Kersten number, and 4) calculate the thermal conductivity.

Dry thermal conductivity. Johansen developed a semiempirical equation to predict the dry thermal conductivity for natural soils:

$$\kappa_{dry} = \frac{0.135\gamma_d + 64.7}{2700 - 0.947\gamma_d}, \tag{6}$$

where κ_{dry} is in W m^{-1} K^{-1}, γ_d is the dry density in kg m^{-3}, and the solids unit weight is taken as 2700 kg m^{-3}. At the FIFE site, dry density was measured, but in practice, the dry density may be obtained from the porosity n assuming the same solids unit weight as

$$\gamma_d = (1 - n)2700. \tag{7}$$

For crushed rock, the dry thermal conductivity is a function of porosity n only:

$$\kappa_{dry} = 0.039n^{-2.2}. \tag{8}$$

Saturated thermal conductivity. The saturated thermal conductivity κ_{sat} for natural soils depends on the porosity n, the quartz content q, and the unfrozen volume fraction

$$\kappa_{sat} = \kappa_s^{1-n}\kappa_i^{n-x_u}\kappa_w^{x_u}, \tag{9}$$

where the thermal conductivity of ice $\kappa_i = 2.2$ W m^{-1} K^{-1}, the thermal conductivity of water $\kappa_w = 0.57$ W m^{-1} K^{-1}, and the solids thermal conductivity κ_s is given as

$$\kappa_s = \kappa_q^q\kappa_o^{1-q}. \tag{10}$$

In the above equation, the thermal conductivity of quartz $\kappa_q = 7.7$ W m^{-1} K^{-1}, and the thermal conductivity of other minerals is given as $\kappa_o = 2.0$ W m^{-1} K^{-1} for $q > 0.2$ and $\kappa_o = 3.0$ W m^{-1} K^{-1} otherwise.

Kersten number. The Kersten number is a function only of the degree of saturation S_r and phase of the water. For unfrozen soils,

$$K_e = \begin{cases} 0.7 \log S_r + 1.0 & S_r > 0.05 \quad \text{coarse} \\ \log S_r + 1.0 & S_r > 0.1 \quad\ \text{fine.} \end{cases} \tag{11}$$

For frozen soils,

$$K_e = S_r. \tag{12}$$

Although the method is extremely simple to code, and the parameters it requires such as porosity, density, and saturation are typically already implemented in SVATS [or readily available as a function of soil texture from Cosby et al. (1984) or Rawls et al. (1982)], the implementation of Johansen's method into SVATS is hampered by the two additional parameters it requires: quartz content and particle size. Below we discuss the parameter requirements of J75 and their associated uncertainties.

c. Estimating parameters in J75

Quartz content. Generally, soil scientists measure the quartz content of a specific soil sample as it is required. Quartz content as a function of soil type is not tabulated. However, it is known that sand usually contains a very high percentage of quartz in crystalline form (Buckman and Brady 1969). Silts and clay may also contain silicates, but these are not generally in the form of crystals. It is only quartz crystals that have a very high thermal conductivity, whereas the conductivity of quartz or silicate material bound inside clay or silt particles is similar to that of other soil materials (Farouki 1986). For the purposes of SVAT modeling, it was assumed that the quartz content for each soil type was related to the percentage of sand in the soil. The quartz content of the sand was allowed to vary from 0% to 100%, and the quartz fraction of the soil therefore to range from zero to the maximum sand content of that soil type, as determined using the United States Department of Agriculture (USDA) soil triangle. Since the likelihood of the sand portion of a soil having a low quartz content is

TABLE 2. Recommended quartz content and maximum expected variation in thermal conductivity (t.c.) from Johansen's method by soil type.

Soil texture	Quartz content	Maximum t.c. variation (%)
Sand	0.92	55.2
Loamy sand	0.82	52.9
Sandy loam	0.60	49.2
Sandy clay loam	0.60	48.4
Sand clay	0.52	46.2
Loam	0.40	35.0
Clay loam	0.35	34.2
Silt loam	0.25	25.1
Clay	0.25	26.8
Silty clay	0.10	17.3
Silty clay loam	0.10	22.9
Silt	0.10	17.3
Peat	0.00	—

rather small, an average value of quartz for the soil type was chosen by assuming that all the sand was composed of quartz for a soil with a median percentage of sand as depicted in the USDA triangle. This analysis led to a set of median quartz contents versus soil texture class as given in Table 2. Since peat is not one of the USDA soil types, we assumed that peat contains no quartz for the purposes of applying J75. Also given in Table 2 is a maximum percentage deviation in thermal conductivity due to uncertainties in all other parameters as discussed below.

Particle size. A soil with more than 5% of material having grain size less than 2 μm is considered "fine" (Farouki 1986). Thermal conductivity calculations assuming both fine and coarse soils at average values of other parameters indicated that the difference in predicted values versus grain size was not significant. In light of the lack of availability of grain size data, we consider all soils to be fine in subsequent analyses.

Porosity. The average values and ranges of porosity by soil type were taken from Rawls et al. (1982), who combined data from 1323 soils to tabulate a variety of soil water properties, including typical soil type porosity and standard deviations. The upper and lower values of porosity used were one standard deviation above and below the given mean effective porosity. Analysis of the relative sources of uncertainty in parameters affecting thermal conductivity estimates indicates that porosity is a more significant factor than quartz content and density.

Dry density. No specific tabulation of dry density ranges for soil types was available. The range in dry density used in the analysis was obtained using Eq. (7) to calculate density from the range in porosity values from Rawls et al. (1982). This approach gave ranges comparable to ranges given for some of Kersten's (1949) reference soils, and to the typical ranges by soil class in Das (1985). The porosity method was not applied to

peat, for which the density came only from Kersten (1949).

Based on the closeness of the average calculated values of Johansen's method to the available data, it is recommended that the median parameter values be used in the absence of specific data. These include the Rawls et al. (1982) porosity values and the dry densities calculated from them and the listing of average quartz content by soil type provided in Table 2. This table also lists the probable maximum range in thermal conductivity predicted by Johansen's method using the maximum and minimum quartz contents, matched with minimum and maximum porosities and dry densities. Since the actual soil parameters may be expected to fall somewhere between the extremes, the error in thermal conductivity should be bounded by these percentages. The largest variation is just over 50%, a significant improvement over the MP81 method, which deviated from the reference values by 300% or more during wet conditions. As these maximum percentages for Johansen's method represent deviations for a soil that varies significantly from the average in each respect, the actual error should be considerably smaller for most soils.

The following section presents an intercomparison of MP81 and J75 thermal conductivity predictions versus various tabulated values and measured values at the FIFE site.

3. Performance intercomparison

a. Tabulated values

A comparison of soil thermal conductivity values predicted by the MP81 and J75 methods to reference tabulated values is shown in Table 3 as well as in Figs. 1–3, where we have made assumptions regarding the soil hydraulic relationships implicitly required by MP81, as well as assumptions regarding the particle size and quartz content required by J75. Both Table 3 and Figs. 1–3 illustrate differences in predicted thermal conductivity versus saturation for sand, clay, and peat, since these soil textures effectively represent the range of differences found between MP81 and J75. In Table 3, we present two columns for MP81, corresponding to differences in soil water retention functions: CH78 for Clapp and Hornberger (1978), and R82 for Rawls et al. (1982). In Figs. 1–3, we show the same reference, MP81 and J75 values as in Table 3, and in Figs. 1 and 2 we show two additional J75 values representing maximum and minimum quartz content values (these are not shown for peat since it contains no quartz). Thus, the additional J75 lines illustrate the uncertainty in the method with respect to quartz content. The table and figures illustrate that the differences between MP81 and tabulated values are large at high moisture levels, and smaller but still significant at low saturations. The differences between MP81 and the reference values depend somewhat on the soil type and which soil hydraulic relationship is

TABLE 3. Comparison of thermal conductivity values. Values of porosity n and quartz content q are given for each soil type. All soils assumed to be fine for J75. Values in W m^{-1} K^{-1}.

Saturation	Reference	MP81 + CH78	MP81 + R82	J75
		Sand ($n = 0.4$, $q = 0.95$)		
0.0	0.30[a]	0.172	0.172	0.240
0.25	1.05[c]	0.833	3.549	1.116
0.5	1.95[c], 1.76[b]	2.818	5.477	1.779
0.75	2.16[c]	5.749	7.059	2.167
1.0	2.20[c], 2.18[b]	9.536	8.451	2.420
		Clay ($n = 0.4$, $q = 0.25$)		
0.0	0.25[a]	0.172	0.172	0.240
0.25	0.63[c]	0.172	0.172	0.724
0.5	1.12[c], 1.17[b]	0.182	0.658	1.090
0.75	1.33[c]	1.358	1.912	1.304
1.0	1.58[c], 1.59[b]	5.643	4.077	1.456
		Peat ($n = 0.8$, $q = 0.0$)		
0.0	0.05[a], 0.06[c]	0.172	—	0.038
0.25	0.13[a]	0.172	—	0.315
0.5	0.22[a], 0.29[c]	0.579	—	0.524
0.75	0.33[a]	2.266	—	0.646
1.0	0.5[a,b,c]	6.435	—	0.733

[a] Farouki (1986).
[b] de Vries (1963).
[c] Pielke (1984).

used, but differences in the range of 300% at saturation are shown for both.

b. FIFE thermal conductivity values

Soil thermal conductivity and gravimetric soil moisture data were collected at 25 FIFE locations after the end of IFC4 on 18 October 1987. Soil thermal conductivity was measured with a hot wire probe at depths of 5 and 10 cm. These data are available on the FIFE CD-ROM (Strebel et al. 1994) along with measured soil parameters such as bulk density and porosity at each location. Both the MP81 (using CH78 parameters) and J75 methods were applied to each location where soil thermal conductivity was collected, with an assumed quartz content of 0.2 at each location. The results of this comparison are presented in Fig. 4, which illustrates modeled versus measured thermal conductivity for each data point. Figure 4 is consistent with the general results from the tabulated values comparison, which indicate that MP81 significantly overpredicts thermal conductivity values for wet areas. The rms error associated with the MP81 method is 1.3 W m^{-1} K^{-1} or about 300%, whereas the rms error for the J75 method is 0.3 W m^{-1} K^{-1} or about 70%.

4. Application to FIFE

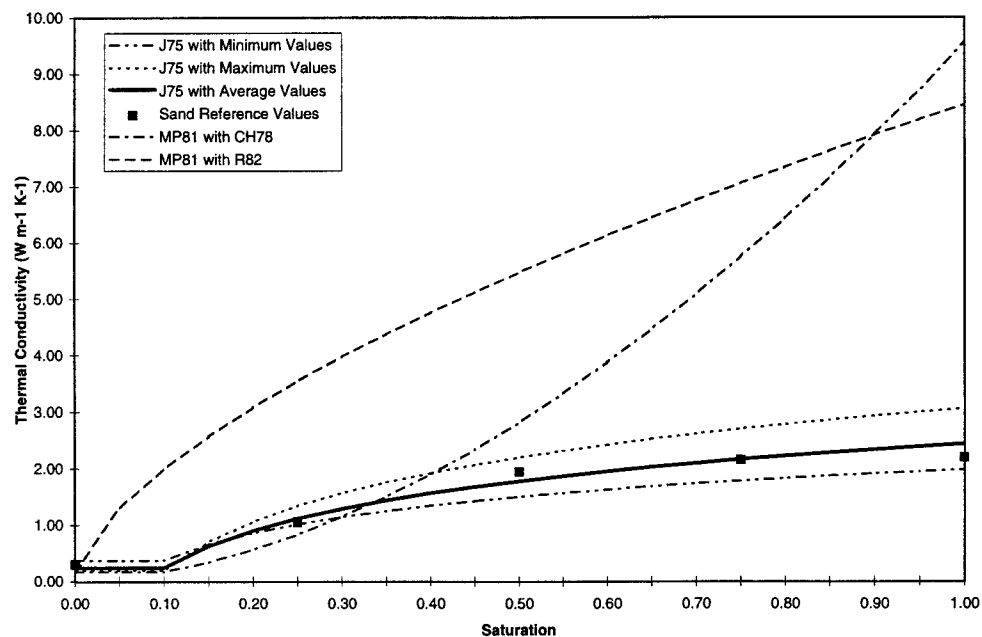Both MP81 and J75 were incorporated into a SVATS and applied to FIFE IFCs 3 and 4. IFC3 took place from

FIG. 1. Thermal conductivity vs saturation for sand. Reference values shown as solid symbols are from Table 3. Curves show values predicted by J75 and MP81 with different assumptions regarding parameters. The solid curve is produced using average quartz content as in Table 2, and parameters related to soil texture from Rawls et al. (1982). The dashed curves produced using J75 show the maximum range in thermal conductivity produced by uncertainties in quartz content. Note that at high and low moistures, the MP81 method produces values that deviate from reference values by up to a factor of 5.
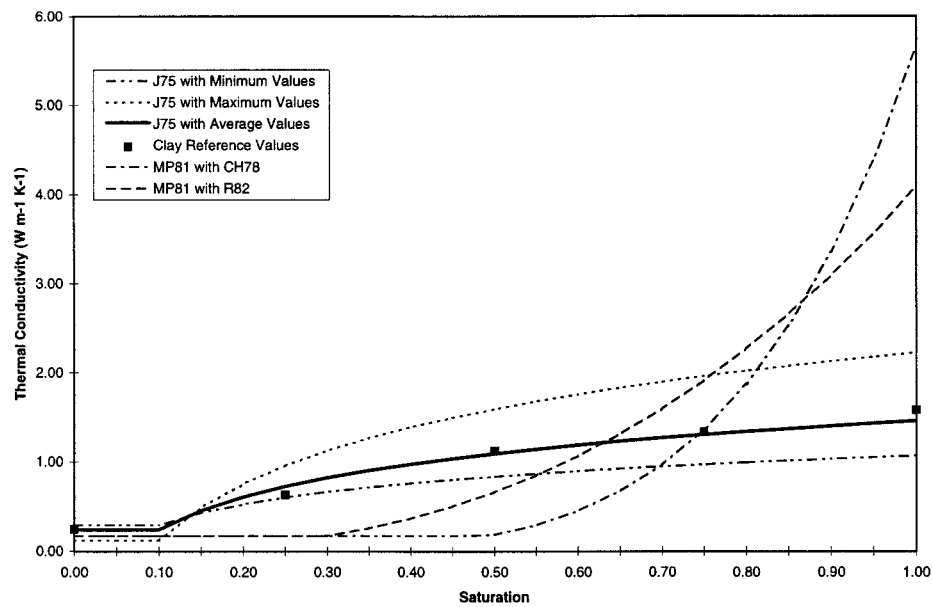
FIG. 2. Same as Fig. 1 but for clay.

6 to 21 August 1987 (day 218–233) and was characterized by wet conditions and intermediate vegetative greenness. IFC4 took place 5–16 October 1987 (day 278–289) and was characterized by dry, senescent conditions. The SVATS is known as TOPLATS (TOP-MODEL-based Land Atmosphere Transfer Scheme) and represents subgrid-scale spatial variability in topography and soils as a distribution and models spatial variability in soil moisture and water table depth, as well as surface fluxes and temperatures by performing separate water and energy balances over each interval of the subgrid soils-topographic distribution. The application of TOPLATS to FIFE is discussed by Famiglietti and Wood (1994a,b) and Peters-Lidard et al. (1997), who have shown that the model successfully simulates the energy balance as well as the temperatures and soil moistures and long-term water balance for the FIFE site. The parameters for the model application in this work are identical to those in Peters-Lidard et al. (1997)

Figures 5 and 6, which are taken from simulations starting in IFC1 as in Peters-Lidard et al. (1997) show that TOPLATS represents the 5-cm soil moisture ob-
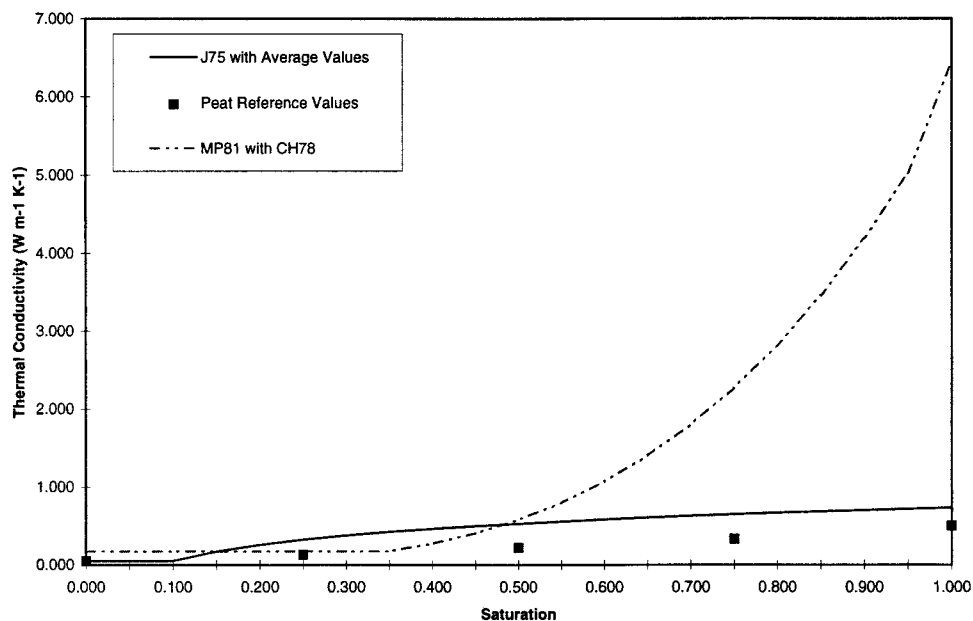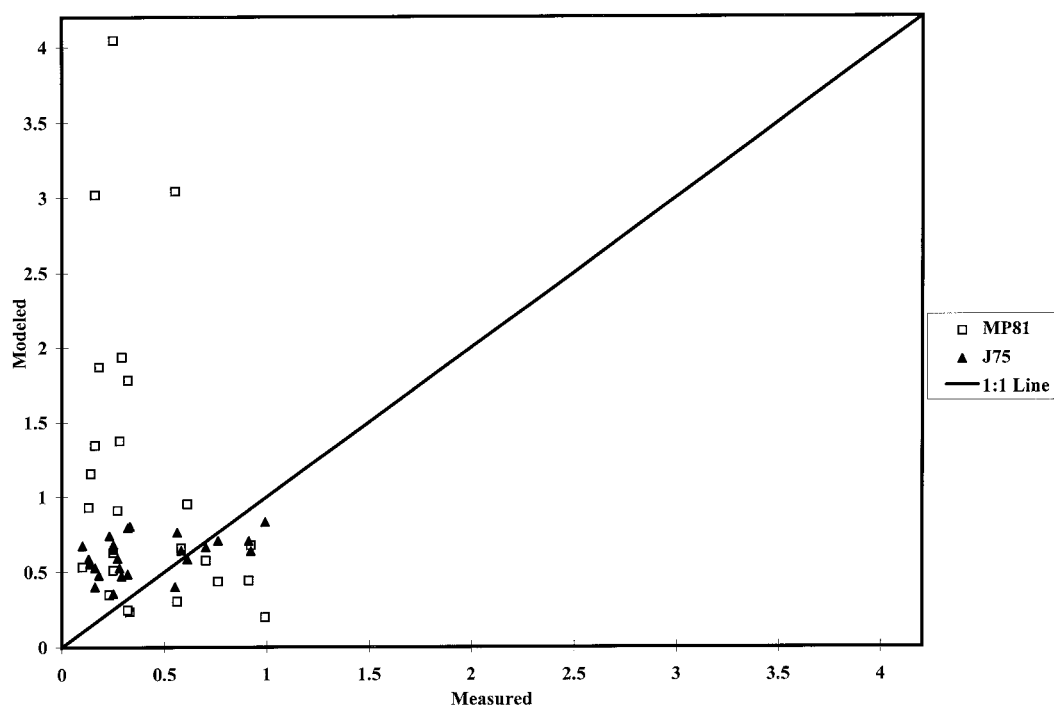

FIG. 3. Same as Fig. 1 but for peat.

FIG. 4. Scatterplots of modeled versus measured soil thermal conductivity for FIFE using MP81 and J75 methods and measured soil moisture. Solid line is 1:1.
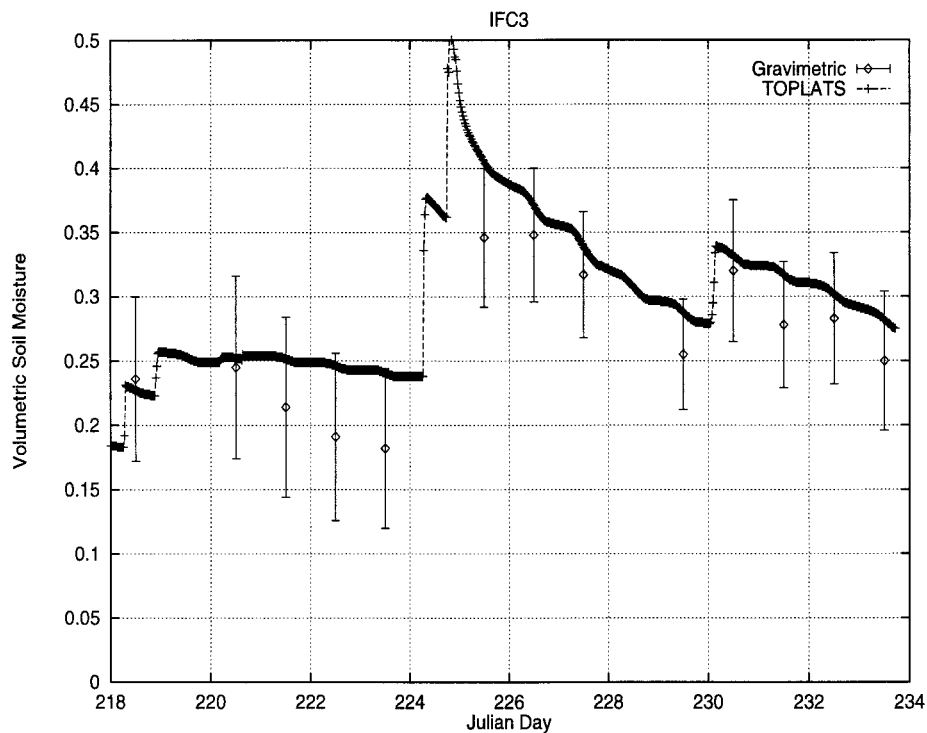

FIG. 5. Time series of TOPLATS modeled and measured average soil moisture for FIFE IFC3. The measurements were converted from gravimetric to volumetric using the measured bulk density. The diamonds represent the average of the converted measurements and the error bars represent one sample standard deviation about the average. The model represents an average over the distribution of subgrid soil moistures.
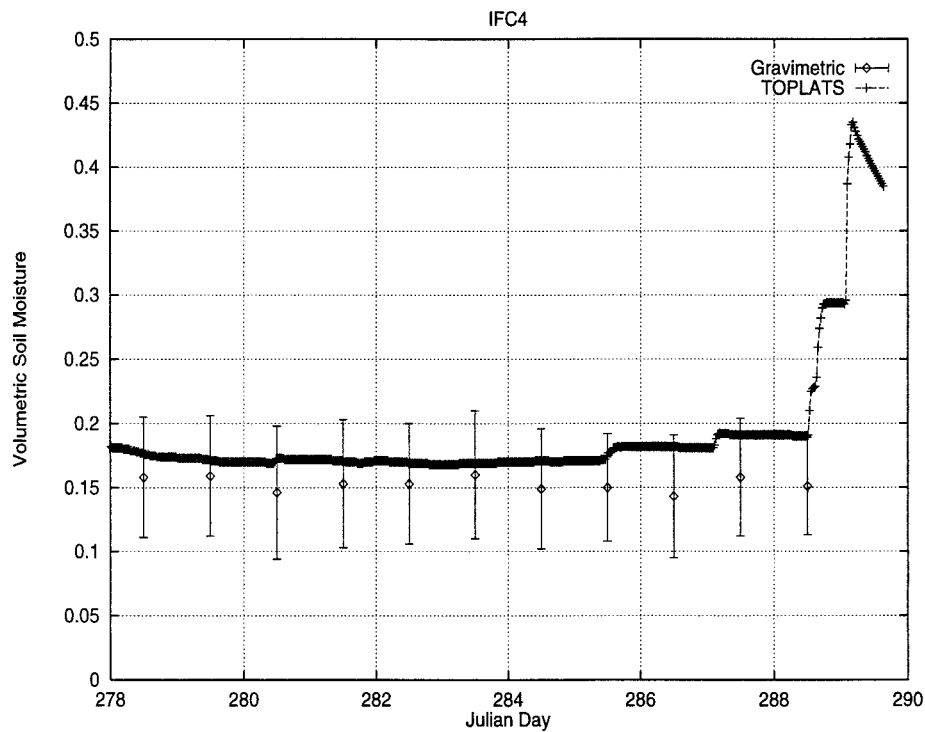
FIG. 6. Same as Fig. 6 but for IFC4.

served in FIFE IFCs 3 and 4 well. Note that we are within the spatial standard deviation of the observations and that we suspect that soil moisture samples from wet areas near the streams are missing from the data.

Given the soil moisture data and simulations of Figs. 5 and 6, which indicate rainfall events in the middle of IFC3 and at the end of IFC4, we next illustrate the effect of soil moisture on the predicted soil thermal conductivity. Both the MP81 and the J75 methods have been implemented in TOPLATS, and Figs. 7 and 8 show time series of predicted thermal conductivity for IFCs 3 and 4, respectively. These figures illustrate both the large range predicted by MP81, which is typically 2–3 times higher than that predicted by J75 during the wet IFC3 and the end of IFC4. Comparison of Figs. 7 and 8 with Figs. 5 and 6 shows the clear relationship between high soil moisture values and large differences in thermal conductivity.

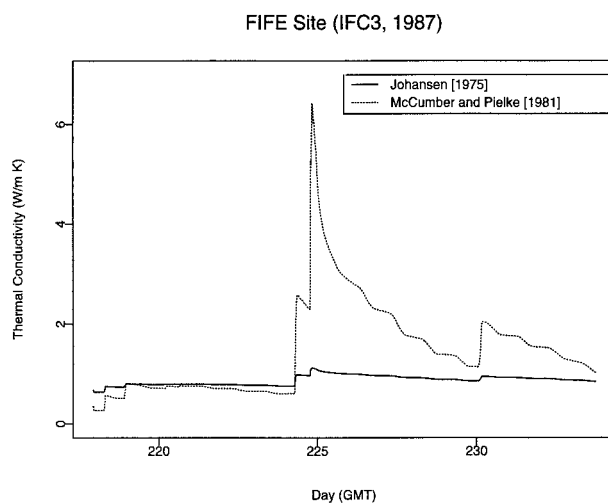Figures 9 and 10 and Table 4 illustrate the perfor-

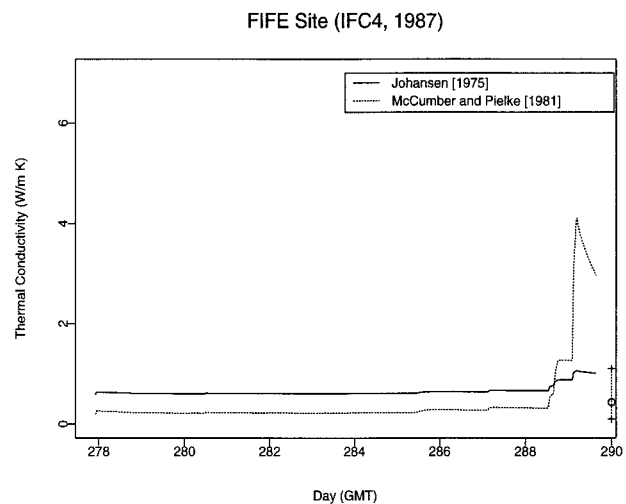FIG. 7. Time series of thermal conductivity predicted by both MP81 and J75 for IFC3.

FIG. 8. Time series of thermal conductivity predicted by both MP81 and J75 for IFC4. Circle indicates mean and crosses indicate minimum and maximum values measured on 18 October 1987.
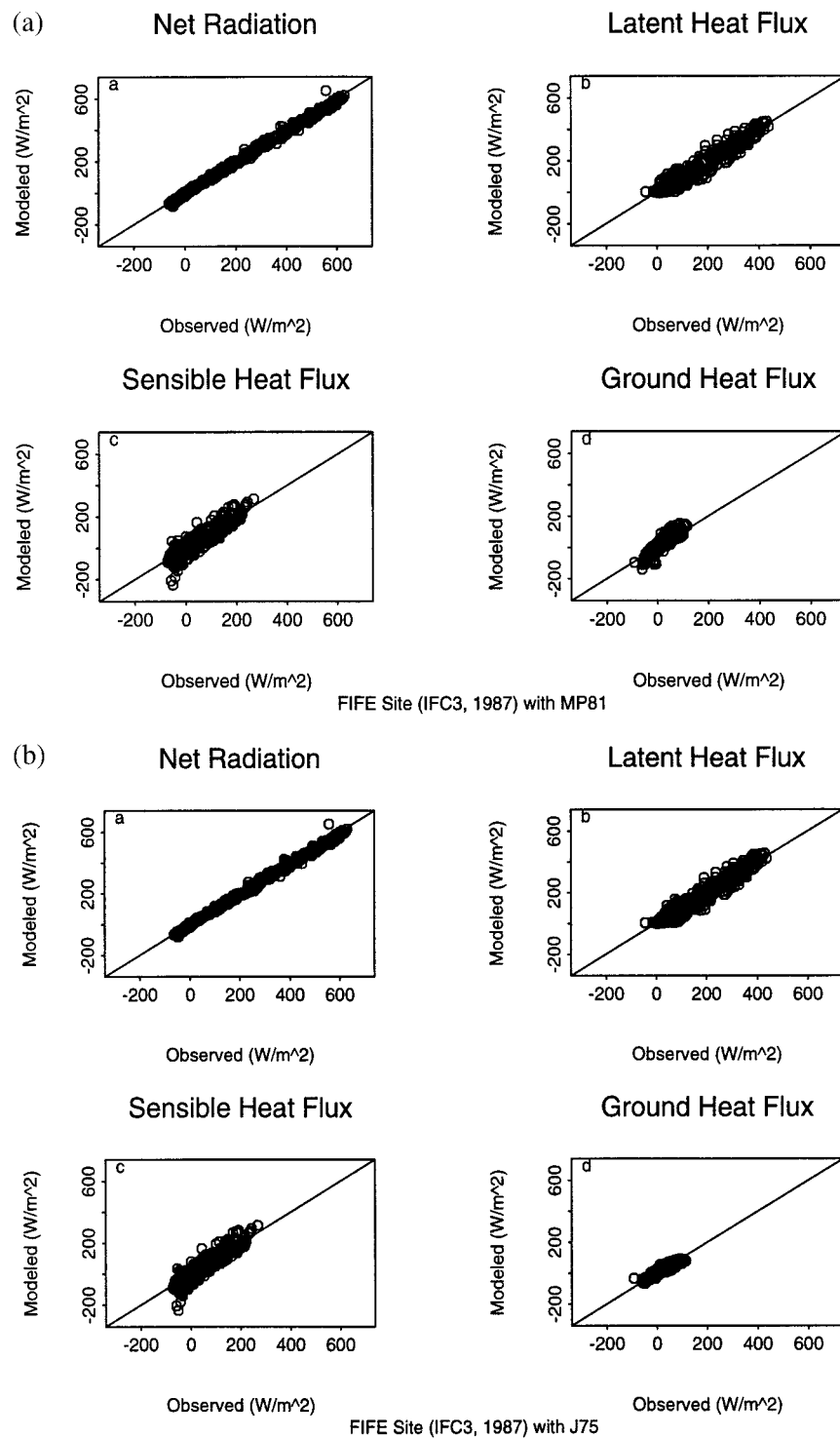
(a)

FIG. 9. Scatterplots of modeled vs measured site average fluxes for FIFE-IFC3 using: (a) MP81 and (b) J75. Solid line is 1:1. Site averages were produced for 30-min intervals by Betts and Ball and are available on the FIFE CD-ROM (Strebel et al. 1994). Model predictions are average fluxes produced by TOPLATS using a distribution to account for subgrid heterogeneity in soil moisture.
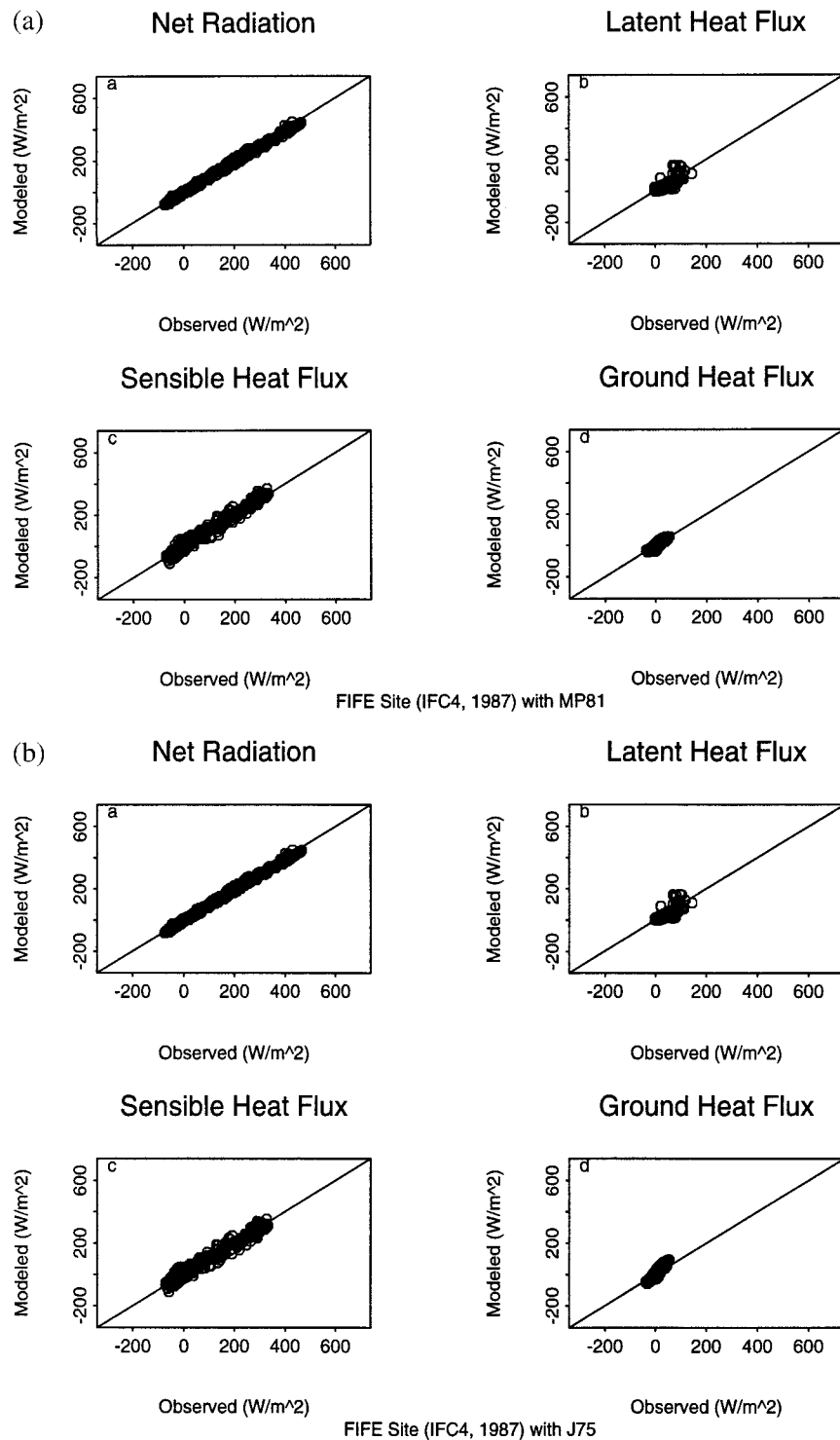
(a)

FIG. 10. Same as Fig. 9 but for IFC4.

mance of TOPLATS predicting the site average energy balance components as computed by Betts and Ball and found on the FIFE CD-ROM (Strebel et al. 1994) for IFCs 3 and 4. Figures 9a and 10a were generated using MP81 while Figs. 9b and 10b were generated using J75. Figures 9a,b illustrate that for the wet IFC3 the ground heat flux is larger than that observed using the MP81 method. Differences are much smaller between Figs.

TABLE 4. Error statistics for TOPLATS using MP81 and J75. Bias and rms error in watts per square meter.

Statistic	IFC3		IFC4	
	MP81	J75	MP81	J75
Net radiation				
Slope	0.99	0.99	0.97	0.98
R-squared	1.00	1.00	1.00	1.00
Bias	−7.7	−7.7	−4.8	−5.4
Rms error	13.9	13.8	11.2	10.9
Latent heat flux				
Slope	1.01	1.03	0.88	0.85
R-squared	0.95	0.96	0.75	0.75
Bias	−8.09	−7.2	−7.26	−7.38
Rms error	27.6	26.8	15.2	15.2
Sensible heat flux				
Slope	1.00	1.07	1.02	0.95
R-squared	0.84	0.87	0.98	0.97
Bias	−0.9	0.1	6.9	5.9
Rms error	31.0	29.9	18.2	20.4
Ground heat flux				
Slope	1.22	0.94	1.1	1.67
R-squared	0.86	0.90	0.91	0.94
Bias	2.3	0.46	−2.8	−2.3
Rms error	21.6	12.7	17.0	8.6

10a and 10b since they represent the relatively dry conditions of IFC4. Table 4 gives the error statistics for components of the spatially averaged energy balance as shown in Figs. 9 and 10. As the figures illustrate, errors in the ground heat flux are generally smaller with the J75 method, as are errors in other components of the energy balance.

Given that the model seems to perform better on average with the J75 method [which is consistent with the findings of Liang et al. (1997, manuscript submitted to *J. Geophys. Res.*) with the VIC Model], next we present Figs. 11a–d, which illustrate the differences in the model-predicted energy balance for IFC3 due to thermal conductivity formulation. As expected, differences are most significant in the ground heat flux term, while these differences seem to partition primarily into the sensible heat flux and also into the latent heat flux. Differences in the net radiation are typically very small (less than 10 W m^{-2}). This is consistent with the findings of Clark and Arritt (1995). The maximum difference in ground heat flux is 101 W m^{-2}, which occurs due to a phase shift in the ground heat flux where the MP81 value is near −50 W m^{-2} and the J75 value is near 50 W m^{-2}. More typical maximum differences at midday are 50–75 W m^{-2}. The maximum absolute differences in sensible and latent heat fluxes for IFC 3 are 74 and 56 W m^{-2}, respectively.

Figures 12a–d illustrate the similar differences for
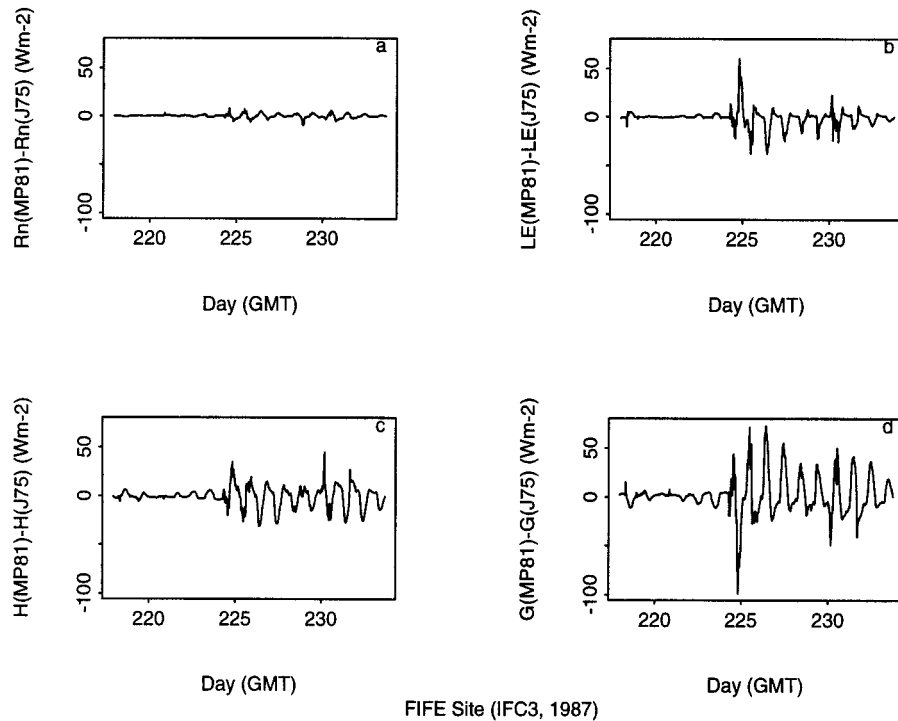

FIFE Site (IFC3, 1987)

FIG. 11. Time series of modeled IFC3 energy flux differences due to thermal conductivity formulation. All values are MP81–J75. The differences show a clear diurnal cycle, are highest following the rainfall events at the beginning and middle of the IFC, and affect mainly the sensible and ground heat fluxes.
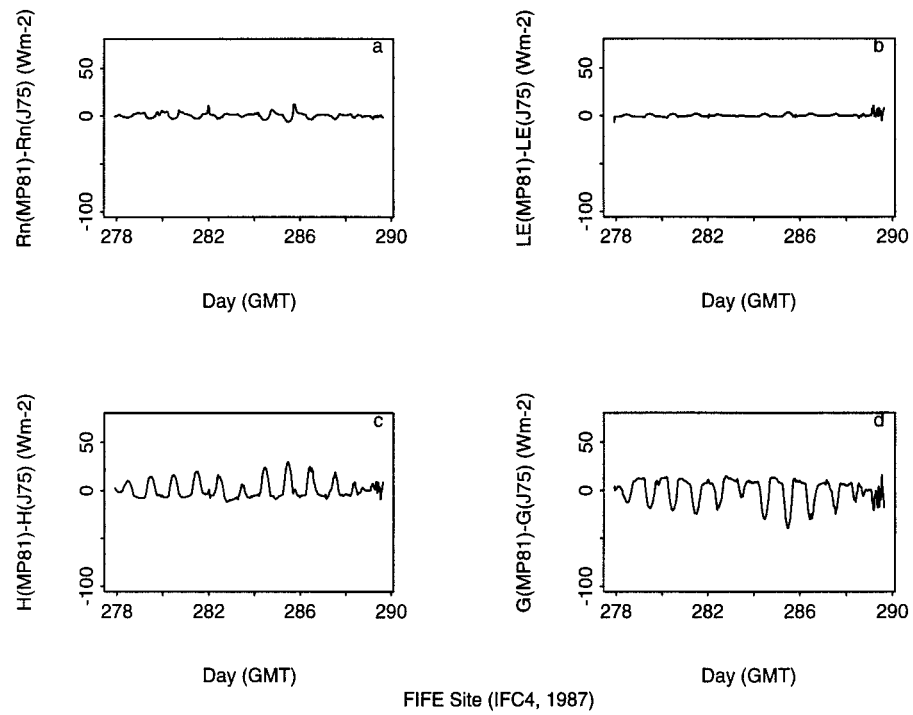
FIG. 12. Time series of modeled IFC4 energy flux differences due to thermal conductivity formulation. All values are MP81–J75. The differences are smaller and of opposite sign to those predicted during IFC3.
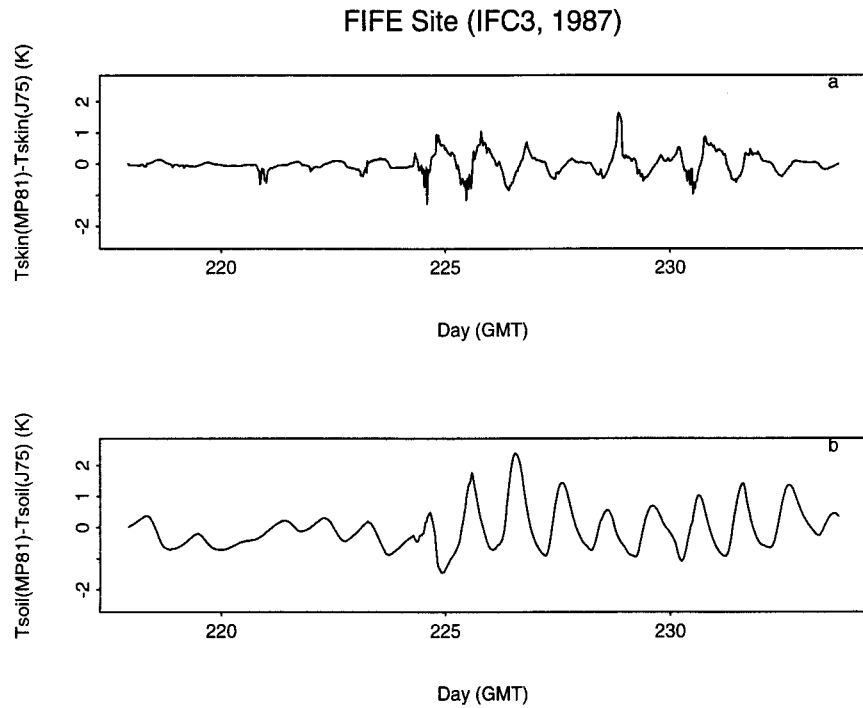
FIFE Site (IFC3, 1987)

FIG. 13. Time series of modeled IFC3 skin and 10-cm soil temperature differences due to thermal conductivity formulation.
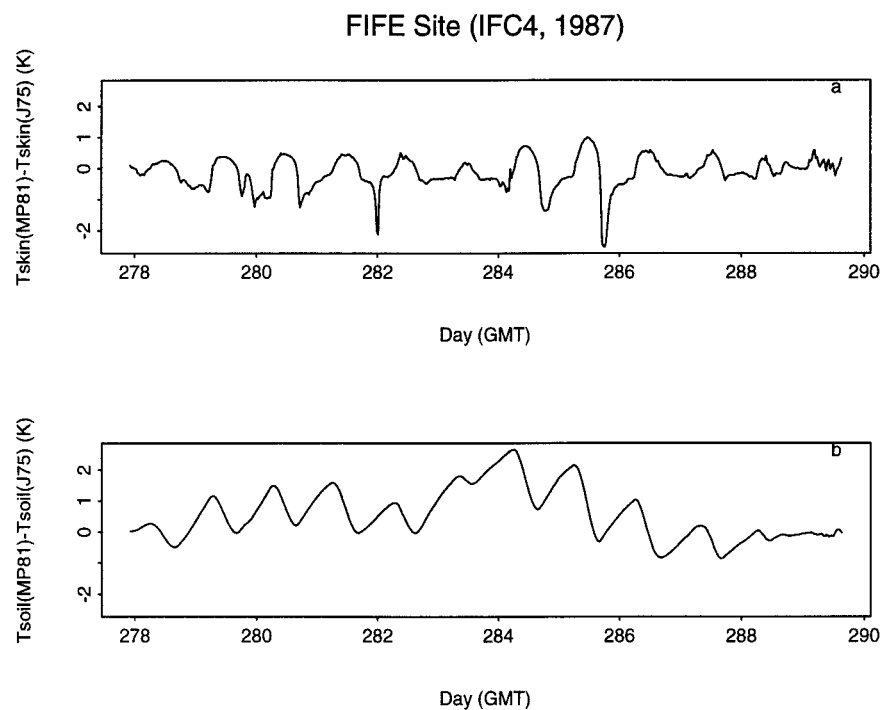
FIFE Site (IFC4, 1987)
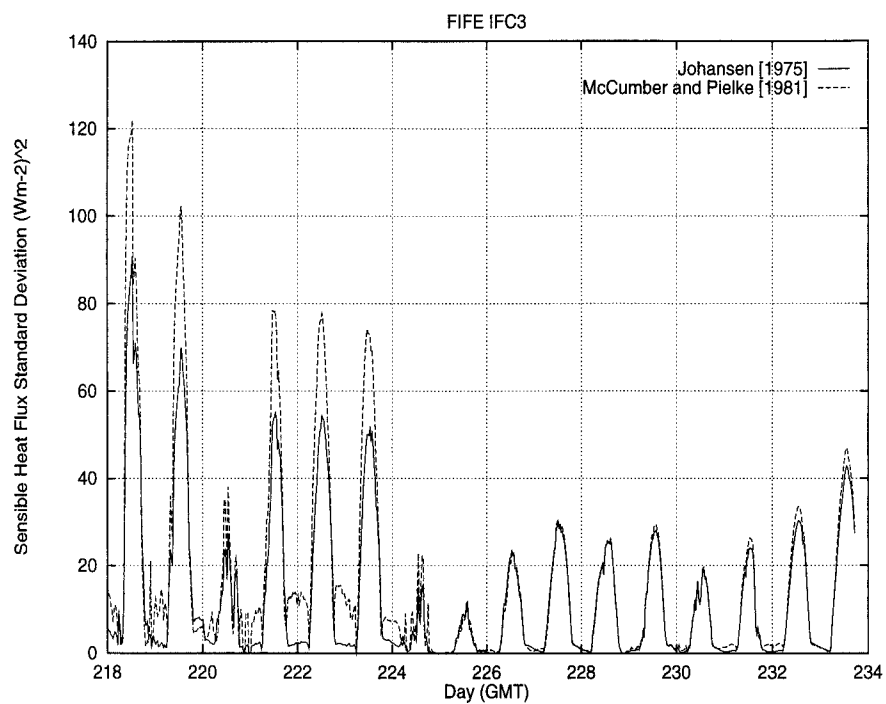

FIG. 14. Same as Fig. 12 but for IFC4.

FIG. 15. Time series of modeled spatial variability in sensible heat flux associated with spatial variability in soil moisture for IFC3. The MP81 method predicts more variability than the J75 method.
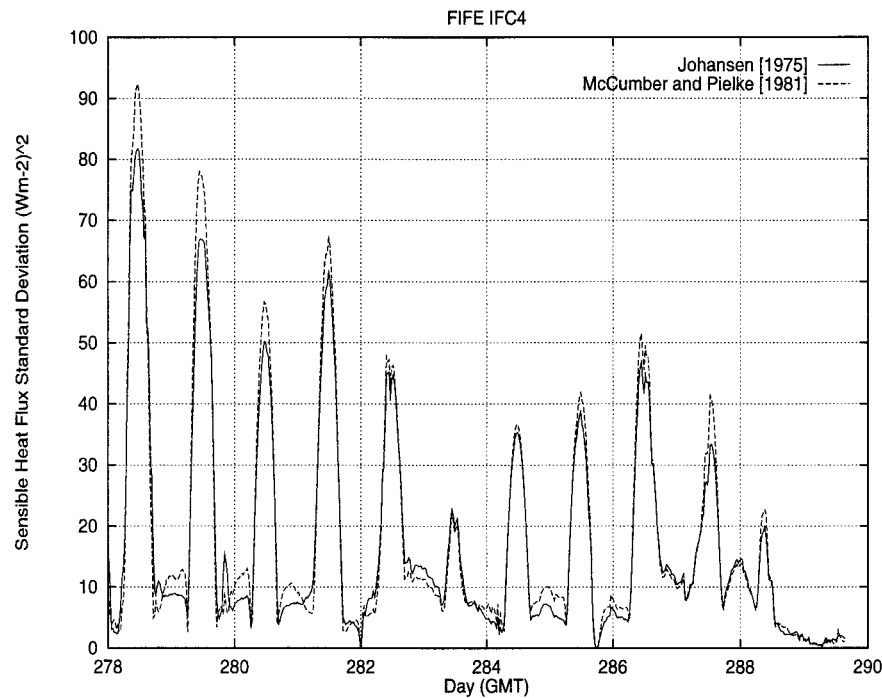
FIG. 16. Same as Fig. 14 but for IFC4.

IFC4. The differences in this case are of a smaller magnitude and of an opposite sign since IFC4 is quite dry, and as discussed previously the MP81 method predicts thermal conductivity values that are too small in dry conditions. The maximum IFC 4 differences shown in Fig. 12 for ground, sensible, and latent heat due to thermal conductivity formulation are 34, 26, and 11 W m^{-2}, respectively.

The most significant differences due to the thermal conductivity formulation are evident in Figs. 13 and 14, which illustrate skin and 7.5-cm soil temperature differences for IFC3 and 4. These differences are typically on the order of 1–2 K, with the maximum differences in skin and soil temperatures of 1.5 and 2.6 K occurring during FIFE IFC3 after the rainfall on 12–13 August (days 224–225). Figures 13 and 14 illustrate that the skin temperature difference is smaller in magnitude and opposite in sign to the soil temperature difference. This partially explains why the differences in energy fluxes and particularly net radiation are smaller relative to the ground heat flux differences. In the daytime during IFC3 we obtain a warmer surface for J75 relative to MP81, whereas for IFC4 we obtain a cooler surface for J75 relative to MP81. Again, this is consistent with the findings of Clark and Arritt (1995), who found increased rainfall over wet surfaces and decreased rainfall over dry surfaces after switching from the MP81 method to another thermal conductivity method.

If one considers temperature differences predicted with SVATS, which incorporate spatial variability in soil moisture, it is conceivable that temperature con-

trasts predicted by the MP81 method would be too high and would thus overestimate the development of circulations due to the induced pressure gradients. Figures 15 and 16 show time series of sensible heat flux spatial variability predicted by solving separate water and energy balances for each interval of the soils-topographic index distribution for IFC3 and IFC4. This produces a distribution of soil moistures and soil temperatures as well as distribution of each flux component. As discussed by Peters-Lidard et al. (1997) these distributions actually underestimate the true variability of surface states and fluxes due to their neglect of rainfall spatial variability and vegetation heterogeneity. However, the figures clearly illustrate the enhancement of spatial variability associated with MP81, relative to the variability predicted with J75. This enhancement is evident mainly in the intermediate wetness time period prior to the rainfall in IFC3, as shown in Fig. 15 (cf. Fig. 11c where the largest mean difference are after the rainfall). Differences in variability are generally less in IFC4 (Fig. 16) due to the drier conditions. Models that include rainfall and/or vegetation variability could produce even bigger differences in spatial sensible heat flux variations, and this has strong implications for past sensitivity studies that have used the MP81 method.

5. Conclusions

The formulation of thermal conductivity has been shown to have a significant impact on the partitioning of surface energy fluxes and the prediction of soil and

skin temperatures in SVATS. In particular, differences of up to 74 W m^{-2} in spatially averaged sensible heat flux and 56 W m^{-2} in spatially averaged latent heat flux were found for FIFE IFC3. In addition, maximum differences in spatially averaged skin and 7.5-cm soil temperatures of 1.5 and 2.6 K were found for FIFE IFC3. These differences increased with moisture content and were smaller in the drier IFC4.

The implementation of Johansen's method into SVATS should provide good estimates for thermal conductivity with the specification of one additional parameter value—the quartz content—as given in Table 2. This method has been shown to be superior to other methods for predicting thermal conductivity of soils, such as de Vries (1963). In addition, as shown with FIFE data, the method produces much more realistic behavior of the saturation–thermal conductivity relationship, which is exaggerated by the McCumber and Pielke (1981) formulation.

The FIFE data have provided a limited test of thermal conductivity parameterizations, and it is recommended that future field experiments take simultaneous thermal conductivity, soil moisture, bulk density, and (if possible) quartz content measurements in order to support additional intercomparisons. In addition, since thermal conductivity exhibits a strong control on the amplitude and phase response of heat diffusion, SVATS that have incorporated the MP81 method should reexamine the implications of this parameterization on their results and model geometries.

REFERENCES

Al Nakshabandi, G., and H. Kohnke, 1965: Thermal conductivity and diffusivity of soils as related to moisture tension and other physical properties. *Agric. Meteor.,* **2,** 271–279.

Avissar, R., and R. A. Pielke, 1989: A parameterization of heterogeneous land surfaces for atmospheric numerical models and its impact on regional meteorology. *Mon. Wea. Rev.,* **117,** 2113–2136.

——, and M. M. Verstraete, 1990: The representation of continental surface processes in atmospheric models. *Rev. Geophys.,* **28,** 35–52.

Buckman, H. O., and N. C. Brady, 1969: *The Nature and Properties of Soils.* MacMillan, 653 pp.

Chen, F., and Coauthors, 1996: Modeling of land surface evaporation by four schemes and comparison with FIFE observations. *J. Geophys. Res.,* **101**(D3), 7251–7268.

Clapp, R. B., and G. M. Hornberger, 1978: Empirical equations for some soil hydraulic properties. *Water Resour. Res.,* **14,** 601–604.

Clark, C. A., and R. W. Arritt, 1995: Numerical simulations of the effect of soil moisture and vegetation cover on the development of deep convection. *J. Appl. Meteor.,* **34,** 2030–2045.

Collins, D. C., and R. Avissar, 1994: An evaluation with the Fourier amplitude sensitivity test (FAST) of which land–surface parameters are of greatest importance in atmospheric modeling. *J. Climate,* **7,** 681–703.

Cosby, B. J., G. M. Hornberger, R. B. Clapp, and T. R. Ginn, 1984: A statistical exploration of the relationship of moisture characteristics to the physical properties of soils. *Water Resour. Res.,* **20,** 682–690.

Cuenca, R. H., M. Ek, and L. Mahrt, 1996: Impact of soil water property parameterization on atmospheric boundary layer simulation. *J. Geophys. Res.,* **101** (D3), 7269–7277.

Das, B. M., 1985: *Principles of Geotechnical Engineering.* PWS Engineering, 571 pp.

Deardorff, J. W., 1978: Efficient prediction of ground surface temperature and moisture, with inclusion of a layer of vegetation. *J. Geophys. Res.,* **83**(C4), 1889–1903.

de Vries, D. A., 1963: Thermal properties of soils. *Physics of Plant Environments,* W. R. van Wijk, Ed., North-Holland, 210–235.

Ek, M., and L. Mahrt, 1991: OSU 1D PBL Model: User's guide, version 1.0.4. Dept. of Atmospheric Sciences, Oregon State University, 120 pp. [Available from Dept. of Atmos. Sci., Oregon State University, Corvallis, OR 97331.]

——, and R. H. Cuenca, 1994: Variation in soil parameters: Implications for modeling surface fluxes and atmospheric boundary layer development. *Bound.-Layer Meteor.,* **70,** 369–383.

Famiglietti, J. F., and E. F. Wood, 1994a: Multiscale modeling of spatially variable water and energy balance processes. *Water Resour. Res.,* **30,** 3061–3078.

——, and ——, 1994b: Application of multiscale water and energy balance models on a tallgrass prairie. *Water Resour. Res.,* **30,** 3079–3093.

Farouki, O. T., 1986: *Thermal Properties of Soils.* Series on Rock and Soil Mechanics, Vol. 11, Trans Tech, 136 pp.

Garratt, J. R., 1993: Sensitivity of climate simulations to land–surface and atmospheric boundary-layer treatments—A review. *J. Climate,* **6,** 419–449.

Henderson-Sellers, A., A. J. Pitman, P. K. Love, P. Irannejad, and T. H. Chen, 1995: The Project for Intercomparison of Land Surface Schemes (PILPS): Phases 2 and 3. *Bull. Amer. Meteor. Soc.,* **76,** 489–503.

Hillel, D., 1980: *Fundamentals of Soil Physics.* Academic Press, 413 pp.

Johansen, O., 1975: Thermal conductivity of soils. Ph.D. thesis, University of Trondheim, 236 pp. [Available from Universitetsbiblioteket i Trondheim, Høgskoleringen 1, 7034 Trondheim, Norway.]

Kersten, M. S., 1949: Thermal properties of soils. University of Minnesota Engineering Experiment Station Bulletin 28, 227 pp. [Available from University of Minnesota Agricultural Experiment Station, St. Paul, MN 55108.]

McCumber, M. C., and R. A. Pielke, 1981: Simulation of the effects of surface fluxes of heat and moisture in a mesoscale numerical model. *J. Geophys. Res.,* **86**(C10), 9929–9938.

McInnes, K. J., 1981: Thermal conductivities of soils from dryland wheat regions of eastern Washington. M.S. thesis, Dept. of Agronomy and Soils, Washington State University, Pullman, WA, 51 pp. [Available from Owen Science Library, Washington State University, Pullman, WA 99163-3200.]

Noilhan, J., and S. Planton, 1989: A simple parameterization of land surface processes for meteorological models. *Mon. Wea. Rev.,* **117,** 536–549.

Peters-Lidard, C. D., M. S. Zion, and E. F. Wood, 1997: A soil–vegetation–atmosphere transfer scheme for modeling spatially variable water and energy balance processes. *J. Geophys. Res.,* **102** (D4), 4303–4324.

Philip, J. R., 1957: Evaporation, and moisture and heat fields in the soil. *J. Meteor.,* **14,** 354–366.

Pleim, J. E., and A. Xu, 1995: Development and testing of a surface flux and planetary boundary layer model for application in mesoscale models. *J. Appl. Meteor.,* **34,** 16–32.

Rawls, W. J., D. L. Brakensiek, and K. E. Saxton, 1982: Estimation of soil water properties. *Trans. Amer. Soc. Agric. Eng.,* **25,** 1316–1320.

Sellers, P. J., F. G. Hall, G. Asrar, D. E. Strebel, and R. E. Murphy, 1992: An overview of the First International Satellite Land Surface Climatology Project (ISLSCP) Field Experiment (FIFE). *J. Geophys. Res.,* **97**(D17), 18 345–18 371.

——, D. A. Randall, G. J. Collatz, J. A. Berry, C. B. Field, D. A. Dazlich, C. Zhang, G. D. Collelo, and L. Bounoua, 1996: A revised land surface parameterization (SiB2) for atmospheric GCMs. Part I: Model formulation. *J. Climate,* **9,** 676–705.

Shukla, J., and Y. Mintz, 1982: Influence of land–surface evapotranspiration on the earth's climate. *Science,* **215,** 1498–1501.

Strebel, D. E., D. Landis, K. F. Huemmrich, and B. W. Meeson, 1994: Collected data of the First ISLSCP Field Experiment. *Surface Observations and Non-Image Data Sets,* Vol. 1, NASA, CD-ROM.

Viterbo, P., and A. C. M. Beljaars, 1995: An improved land surface parameterization scheme in the ECMWF model and its validation. *J. Climate,* **8,** 2716–2748.

Walker, J., and P. R. Rowntree, 1977: The effect of soil moisture on circulation and rainfall in a tropical model. *Quart. J. Roy. Meteor. Soc.,* **103,** 29–46.

Xinmei, H., and T. J. Lyons, 1995: The simulation of surface heat fluxes in a land surface–atmosphere model. *J. Appl. Meteor.,* **34,** 1099–1111.